

# Performance Characteristics of a Cluster of 5 kW Laboratory Hall Thrusters

Mitchell L. R. Walker\* and Alec D. Gallimore.†

*Plasmadynamics and Electric Propulsion Laboratory,  
Department of Aerospace Engineering, University of Michigan,  
Ann Arbor, MI 48109 USA  
Phone: 734-936-0541  
Fax: 734-763-0578*

The University of Michigan and United States Air Force Research Laboratory have jointly created a cluster composed of two P5 Hall effect thrusters. The P5 is a 5 kW class laboratory model Hall thruster developed to investigate a thruster similar to that specified by Integrated High Payoff Rocket Propulsion Technology (IHPRT) goals. In this study, the performance characteristics of each of the P5 Hall thrusters are measured in the Large Vacuum Test Facility (LVTF) at the University of Michigan at three facility pumping speeds. The thrusters are evaluated over the range of 300 - 600 V at 5.25 mg/s and 10.46 mg/s. The two thrusters are then operated simultaneously and the thrust of the cluster is measured over the same thruster operating conditions. Analysis of the monolithic thrust measurements shows that as the facility backpressure increases, the thruster discharge current and thrust increase because more background xenon gas is ingested into the thruster discharge chamber. The percent difference between the measured cluster thrust and the sum of the thrust measured for each monolithic thruster for the 10.46 mg/s anode flow rate varies from 11% to 16% as the operating pressure varies from  $5.3 \times 10^{-6}$  Torr to  $2.8 \times 10^{-5}$  Torr. This is greater than the percent difference in thrust for the 5.25 mg/s flow rate, which varies from 0% to 6% as the operating pressure varies from  $3.5 \times 10^{-6}$  Torr to  $1.5 \times 10^{-5}$  Torr. This difference is caused by the ingestion of background gas and thus, the difference in thrust decreases as the cluster operating pressure decreases. In addition, the anode efficiency and specific impulse of the cluster is greater than that of a single monolithic thruster. Comparison of the performance characteristics of the cluster and the monolithic thruster for conditions of nearly equal operating pressure shows that for the 5.25 mg/s anode flow rate the cluster thrust is simply the addition of the two monolithic thrusters. In addition, the anode efficiency and specific impulse are approximately equal to that of the monolithic thruster. These trends do not hold at the 10.46 mg/s anode flow rate for conditions of equal operating pressure because each cluster element elevates the operating pressure in the immediate vicinity of the adjacent thruster.

## I. Introduction

The combination of high specific impulse, high thrust efficiency, and high thrust density makes the Closed-Drift Hall thruster (CDT) appealing for a number of earth-orbit space missions. CDTs can satisfy many of the spacecraft propulsion needs of the United States Air Force (USAF), NASA, and industrial satellite producers for the next several decades. The USAF has recently identified the high-power 50-150 kW CDT propulsion system as the baseline approach for a variety of missions.<sup>1</sup> NASA has recently announced Project Prometheus, which is developing nuclear reactor technology and high-power electric propulsion systems.<sup>2</sup> Next generation communication satellites are becoming both larger and more powerful. Recent satellite designs suggests that electric propulsion

---

\* Graduate Student Researcher, Plasmadynamics and Electric Propulsion Laboratory, Department of Aerospace Engineering, 1052 FXB Building, 1320 Beal Avenue. Student Member AIAA.

† Professor, Plasmadynamics and Electric Propulsion Laboratory, Department of Aerospace Engineering, 3037 FXB Building, 1320 Beal Avenue. Associate Fellow AIAA.

systems will have to double or triple in power from the current 3-5 kW systems within the next decade to satisfy commercial spacecraft needs. This means that vacuum systems will have to be modified to handle the added propellant flow rates demanded by these higher-power thrusters. Many national electric propulsion test facilities, while physically large enough to test 50 kW thrusters, possess pumping speeds that are at least an order of magnitude too low to ameliorate facility pressure effects for plume/contamination, and life testing.

If the tank pressure is too high, the background gas can artificially modify the exhaust plume as well as alter the operation of the CDT itself.<sup>3, 4</sup> Thruster operation may be influenced by entrainment and/or ingestion of the background chamber molecules. This effect artificially increases the propellant mass flow rate of the engine, resulting in performance and operation changes consistent with the increased number of propellant particles. Furthermore, plume diagnostic experiments can be affected. A large partial pressure of background gas molecules can affect ion current density and energy distribution measurements by artificially increasing the local charge density through charge exchange collisions.<sup>5</sup>

While the U. S. Air Force Research Laboratory (AFRL), NASA Glenn Research Center (GRC), and laboratories in Europe have recently upgraded their pumping systems in anticipation of higher-powered thrusters. Vacuum facilities capable of testing 100-plus-kW CDTs are unlikely to be available. Thus, modular, high-power CDT propulsion systems will undoubtedly be required both for USAF and NASA missions in the future to make ground testing feasible.

In response to this issue, the USAF has embarked on the concept of clustering to reach its high power goal; *i.e.*, the use of smaller Hall thrusters in a propulsion array.<sup>6</sup> This would allow a single, smaller Hall thruster that can be analyzed with ground-based testing to be used in the cluster. A cluster of thrusters will have a lower total efficiency and higher dry mass than a monolithic device of equal power. Yet, a cluster provides propulsion system redundancy and the ability to vary the system power while allowing the thrusters in use to operate at their peak efficiency. Moreover, a cluster is more likely to provide higher performance over a wider range of power than a monolithic engine given the modular nature of the former.

The work presented here is directed at the development of a Hall thruster cluster test facility centered around the University of Michigan Large Vacuum Test Facility.<sup>7, 8, 9</sup> A 2x1 cluster of UM/AFRL P5, 5-kW Hall thrusters have been constructed at the University of Michigan. This cluster facilitates the investigation of high-power Hall thruster operation and provides insight into how chamber effects influence monolithic and cluster characteristics. The goal of this work is to measure the thrust of the 2x1 cluster of P5 Hall thrusters. In this study, the thrust of each of the P5 Hall thrusters is measured over the range of 300 - 600 V at 5.25 mg/s and 10.46 mg/s. The two thrusters are then operated simultaneously and the thrust of the cluster is measured over the same thruster operating conditions. In addition, the effect of facility backpressure on Hall thruster performance is quantified.

## II. Experimental Apparatus

### A. Vacuum Facility

All experiments are conducted in the LVTF, shown schematically in Figure 1. The thrusters are mounted at thruster station 1. The LVTF is a stainless steel clad vacuum chamber that has a diameter of 6 m and a length of 9 m. Two blowers, each with a pumping speed of 940 l/s, and four 190 l/s mechanical pumps evacuate the LVTF to moderate vacuum 4 – 13 Pa. To reach high vacuum, the LVTF is equipped with seven CVI TM-1200 re-entrant cryopumps, each of which is surrounded by a LN<sub>2</sub> baffle. The combined pumping speed of the facility is 500,000 l/s on air, and 240,000 l/s on xenon with a base pressure of  $2.7 \times 10^{-5}$  Pa ( $2 \times 10^{-7}$  Torr). At the average anode flow rates investigated—5.25 and 10.46 mg/s, both with a 0.92 mg/s cathode flow—and at nominal xenon pumping speeds of 70,000 l/s, 140,000 l/s, and 240,000 l/s, the operating pressures of the LVTF range from  $4.6 \times 10^{-4}$  Pa ( $3.5 \times 10^{-6}$  Torr) to  $3.8 \times 10^{-3}$  Pa ( $2.8 \times 10^{-5}$  Torr) on xenon. Table 1 shows the LVTF operating pressure for each flow rate at the nominal xenon pumping speeds of 70,000 l/s, 140,000 l/s, and 240,000 l/s. A previous study shows that the nude gauge reading is a much better estimate of the true chamber pressure.<sup>10</sup> The chamber pressures listed in Table 1 are the indicated pressures from the nude gauge, corrected for xenon.

**Table 1** – LVTF background pressure for the investigated flow rates and pumping speeds.

Thruster	Anode (mg/s)	Cathode (mg/s)	Pressure (Torr-Xe)	Pressure (Pa-Xe)	Nominal Pumping Speed
Monolithic	5.25	0.92	9.1E-06	1.2E-03	70,000
Cluster	5.25	0.92	1.5E-05	2.0E-03	70,000
Monolithic	10.46	0.92	1.4E-05	1.9E-03	70,000
Cluster	10.46	0.92	2.8E-05	3.7E-03	70,000
Monolithic	5.25	0.92	5.3E-06	7.1E-04	140,000
Cluster	5.25	0.92	8.6E-06	1.1E-03	140,000
Monolithic	10.46	0.92	8.1E-06	1.1E-03	140,000
Cluster	10.46	0.92	1.3E-05	1.7E-03	140,000
Monolithic	5.25	0.92	3.5E-06	4.7E-04	240,000
Cluster	5.25	0.92	5.4E-06	7.2E-04	240,000
Monolithic	10.46	0.92	5.3E-06	7.1E-04	240,000
Cluster	10.46	0.92	8.9E-06	1.2E-03	240,000

Chamber pressure is monitored by two hot-cathode ionization gauges, as indicated in Fig. 1. The first gauge is a Varian model Bayard-Alpert (BA) gauge with a HPS model 919 Hot Cathode Controller. The BA model 571 ionization gauge is connected to the chamber via a 25-cm-long, by 3.48-cm-inner-diameter, tube. The second is a Varian model UHV-24 nude gauge with a Varian UHV senTorr Vacuum Gauge Controller. The UHV-24 nude gauge is calibrated for air by the manufacturer. Pressure measurements from both gauges are corrected for xenon using the known base pressure on air and a correction factor of 2.87 for xenon according to the following equation<sup>11</sup>

$$P_c = \frac{P_i - P_b}{2.87} + P_b, \quad (1)$$

where  $P_c$  is the corrected pressure on xenon,  $P_b$  is the base pressure, and  $P_i$  is the indicated pressure when xenon is flowing into the vacuum chamber. The corrected nude gauge pressure is reported as the chamber background pressure.

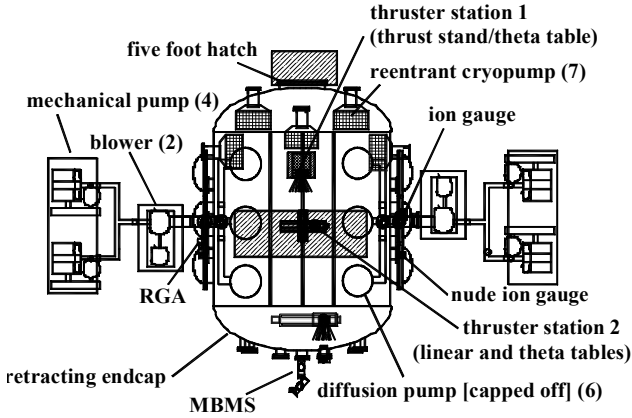


**Figure 1** – Schematic of the LVTF.

A more detailed description of the P5 can be found in Ref. 12.

Each of the P5 Hall thrusters is powered by a separate set of power supplies and operates from its own cathode. The thruster electrical connections enter the chamber through two separate feedthrough ports. Each thruster discharge supply is connected to a filter consisting of a 1.3  $\Omega$  resistance in series with the discharge current and a 95  $\mu\text{F}$  capacitor in parallel. The filter provides isolation of the discharge power supply from the discharge oscillations of the plasma and insures that any oscillations are not a product of feedback between the power supplies and plasma. Discharge current oscillations are measured with a F.W. Bell IHA-25 Hall effect current sensor connected to a Tektronix TDS 3034B oscilloscope.

## B. Hall Thruster

All experiments are performed on the AFRL/UM P5 2x1 cluster of laboratory-model Hall thrusters shown in Figure 2. The P5 has a mean diameter of 148 mm, a channel width of 25 mm, a channel depth of 38 mm, and has a nominal power rating of 5 kW. Laboratory model cathodes are located at the 12 o'clock position on each of the thrusters. The cathode orifice is located approximately 30 mm downstream from the outer front pole piece. For all cases the cathode flow rate is set at 0.92 mg/s. The original P5 discharge channel is machined from M grade boron nitride. The discharge chambers of the cluster elements use the less expensive HP grade boron nitride. A more

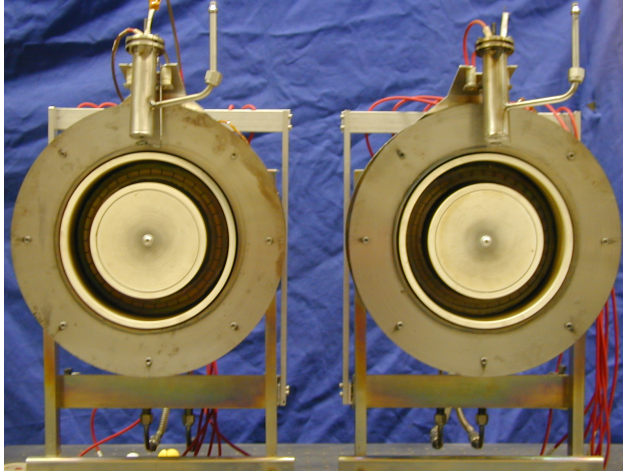


**Figure 2** – UM/AFRL 2x1 5 kW P5 Hall Thruster Cluster.

High-purity (99.9995% pure) xenon propellant is supplied to the Hall thrusters from compressed gas bottles through stainless-steel feed lines. MKS 1179JA mass flow controllers meter the anode and cathode propellant flows. The flow controllers are calibrated with a custom apparatus that measures gas pressure and temperature as a function of time in an evacuated chamber of known volume. The mass flow controllers have an accuracy of  $\pm 1\%$  full scale.

### C. Thrust Stand

Thrust is measured with a high-power null-type inverted pendulum type thrust stand based on the NASA GRC design, the industry standard. The springs of the stand are made with extra stiffness to accommodate the weight of high-power thrusters. The null-type thrust stand holds the thruster at a set position at all thrust levels, which reduces error in the

thrust by eliminating changes in the elevation of the thrust vector. The designer reports the error of the thrust stand to be no better than  $\pm 1\%$  of the full-scale calibration. The uncertainty of the thrust measurements in this experiment, determined by examination of the hysteresis and drift, is  $\pm 1$  mN.

In-situ thruster/thrust-stand leveling is performed with a remotely-controlled geared DC motor coupled to a jackscrew. A remotely-controlled geared DC motor driven pulley system is employed to provide in-situ thrust stand calibration by loading and off-loading small weights to simulate thrust, before and after each test point. A linear curve-fit of null-coil voltage versus thrust is then obtained and used for performance measurements. Soon after the thruster is turned off, a post-test calibration is performed. Current is passed through each set of thruster magnetic coils, and magnetic tares are found to be negligible. Xenon is passed through both of the cathodes, and the cold flow tares are also found to be negligible. This is expected because the cathode centerlines are inclined approximately  $45^\circ$  below the horizontal.

To maintain thermal equilibrium within the thrust stand at Hall thruster operating conditions of 50+ kW, the stand is actively cooled with a VWR International 1172 refrigerated recirculating chiller. The thrust stand cooling consists of two and one-half parallel cooling circuits that travel through the structure and outer radiation shroud.

### D. Cluster Spacing

One of the most important criteria for Hall thruster clustering is the spacing of the array elements. To minimize structural mass and the physical envelope of the cluster the elements of the cluster should be as close as possible without adversely affecting their performance. In large part, the magnetic field inside the Hall thruster channel governs the performance of the Hall thruster.<sup>13</sup> The cluster elements are spaced 40 cm apart (centerline-to-centerline), to ensure that the magnetic field within the discharge chamber and the external radial field are unaffected by the adjacent element of the cluster array at the maximum magnetic field strength operating condition of the monolithic thruster. The maximum magnetic field operating condition has an inner coil current of 8.53 A and an outer coil current of 2.05 A. The radial spacing of 40 cm is selected by measuring the radial magnetic field of one thruster and then of the cluster while increasing centerline spacing. The differences in the radial component of the magnetic field between these two configurations are found to be negligible with a centerline spacing of 40 cm. The magnetic field is measured 6 mm upstream of the thruster exit plane with a standard Hall probe mounted on a linear motion table to provide linear axial position with an accuracy of  $\pm 1$  mm. The error in the magnetic field strength measurement is  $\pm 5\%$ .

The electric fields within the plume plasma are also considered for thruster element spacing. The magnitude of the plasma potential in the plume is not large enough to create an electric field sufficient to cause a substantial deviation in the trajectory of high-speed ions created in the discharge channel. Therefore plume interaction should not be large enough to affect the performance of the individual elements. However, weak electric fields in the plume may alter the plume by changing the trajectories of the slow CEX ions.<sup>8</sup> This effect is not investigated in this paper.

### III. Experimental Results

The primary goal of this study is to compare the performance of a single thruster element to the cluster array. First, the performance of each thruster is measured separately to ensure that the thrusters are nearly identical. Next, the performance of the cluster is measured with both engines operating at anode flow rates of 5.25 mg/s and 10.46 mg/s over a discharge voltage range of 300 - 600 V. To investigate the effect of facility background pressure, the performance of the monolithic thrusters and cluster are measured at backpressure of  $3.5 \times 10^{-6}$  Torr to  $1.4 \times 10^{-5}$  Torr. Tables 2 and 3 present the operating conditions at which the monolithic thrusters (P5-A and P5-B) are investigated. Table 4 presents the operating conditions at which the cluster is investigated.

#### Performance

The effect of facility backpressure on Hall thruster performance is investigated by measuring the performance of the P5-A and P5-B at three pumping speeds. Tables 2 and 3 show that the anode mass flow rate and magnet settings remain constant at each power setting across the three pumping speeds. As the facility backpressure increases, the thruster discharge current and thrust increase as more background xenon gas is ingested into the thruster discharge chamber. All performance parameters presented in this paper exclude the cathode.

Figures 3 and 4 present the measured thrust of the P5-A and P5-B, respectively, as a function of discharge voltage for anode flow rates of 5.25 mg/s and 10.46 mg/s. The thrust produced by each of the monolithic thrusters is nearly identical and increases with increasing backpressure, as expected. The agreement gives confidence in the construction of the cluster elements. Figures 3 and 4 also show that the performances of the P5-A and P5-B are close to the original P5 Hall thruster within the error of the thrust measurement.<sup>12, 14</sup> This verifies that the thrusters are assembled similarly to the original P5 Hall thruster.<sup>12</sup>

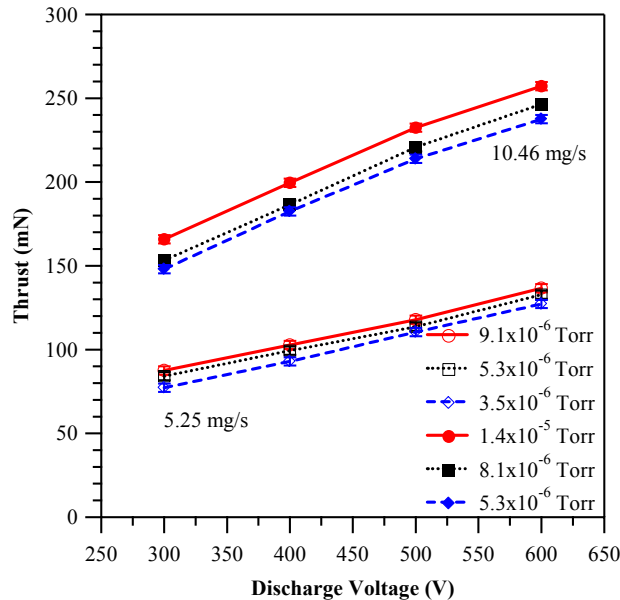


**Figure 3** – The P5-A thrust measurements at anode flow rates of 5.25 mg/s and 10.46 mg/s as a function of discharge voltage at nominal pumping speeds of 70 kl/s, 140 kl/s, and 240 kl/s.

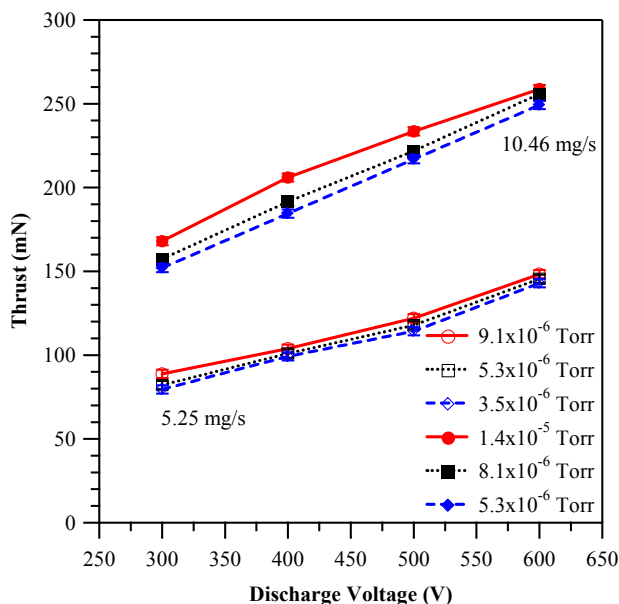


**Figure 4** – The P5-B thrust measurements at anode flow rates of 5.25 mg/s and 10.46 mg/s as a function of discharge voltage at nominal pumping speeds of 70 kl/s, 140 kl/s, and 240 kl/s.

The performance of the cluster is measured after the cluster elements are characterized. Figure 5 shows that thrust of the cluster increases as the facility backpressure increases, as was seen with the monolithic thruster. This is due to the ingestion of neutral background gas into the discharge chambers. Table 4 shows the cluster operating conditions at which performance measurements are taken. These data are discussed in more detail in the next section. It is not possible to measure the performance of the cluster at the upper facility operating pressures and discharge voltages. We believe this is because of the elevated facility backpressure in the immediate vicinity of the exit plane of each thruster. As the facility backpressure increases, the discharge current and the amplitude of the discharge current oscillations increase as the background gas is ingested into the discharge chamber. At the upper facility operating pressures the instability in the discharge current becomes more severe as the discharge voltage is increased for constant backpressure. The amplitude of the discharge current oscillations increases in magnitude as the backpressure increases until there is a disruption in the discharge. In addition, as the thruster approaches the discharge voltage disruption condition, portions of the inner channel begin to glow orange. It appears that the ingested background gas and consequent discharge oscillations enhance the thermal conductivity to the boron nitride channel walls.

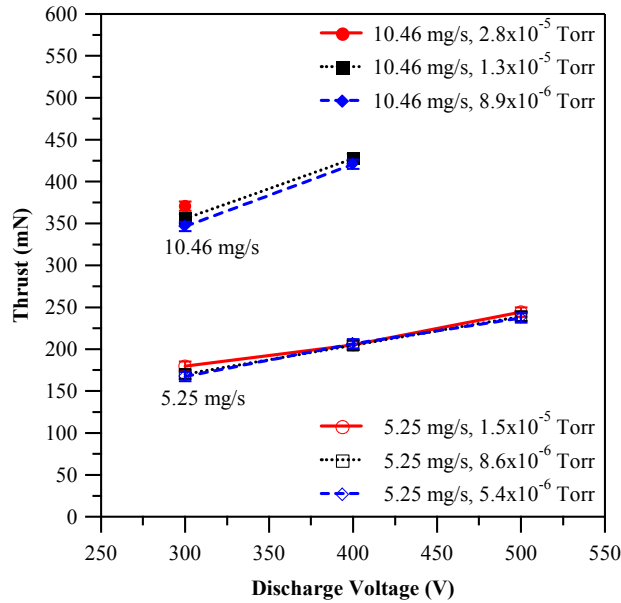


**Figure 5** – Cluster thrust measurements at anode flow rates of 5.25 mg/s and 10.46 mg/s as a function of discharge voltage at nominal pumping speeds of 70 kl/s, 140 kl/s, and 240 kl/s.

### Discharge Current

The time varying discharge current of each of the Hall thrusters and the cluster is measured at each operating condition with an oscilloscope. All discharge current measurements are made after the thrusters have operated for a minimum of one hour.

Figures 6 - 8 present samples of the discharge current oscillations of the monolithic thruster and the cluster. Fast Fourier transforms of these discharge current signals show that the discharge is composed of oscillation frequencies of 0.85 to 10.4 kHz, which are characteristic of Hall thruster operation.<sup>14</sup> Figure 6 shows the nominal discharge current oscillations of the P5-A operating at 300 V, 4.92 A at an operating pressure of  $4.6 \times 10^{-4}$  Pa ( $3.5 \times 10^{-6}$  Torr). The amplitude of the oscillations is approximately 17% of the average discharge current. Figure 7 shows the discharge current of the cluster elements with the P5-A operating at 300 V, 5.14 A and the P5-B operating at 300 V, 4.96 A at an operating pressure of  $7.2 \times 10^{-4}$  Pa ( $5.4 \times 10^{-6}$  Torr). The cluster operates well at this condition, but the amplitude of the discharge current oscillations of the P5-A has increased to 22% of the average discharge current because of the increase in facility backpressure. The amplitude of the P5-B is approximately 14% of the average discharge current. The difference between the P5-A and P5-B oscillation amplitudes may be caused by varying component material properties and assembly tolerances typical of hand-built thrusters, cathodes, and discharge filters. Figure 8 shows the discharge current of the cluster with the P5-A operating at 300 V, 5.76 A and the P5-B operating at 300 V, 5.68 A at an operating pressure of  $3.7 \times 10^{-3}$  Pa ( $2.8 \times 10^{-5}$  Torr). The discharge currents have increased from the values measured at the  $7.2 \times 10^{-4}$  Pa operating pressure. Furthermore, the amplitudes of the discharge oscillations have increased to approximately 37% of the discharge current for both the P5-A and P5-B.

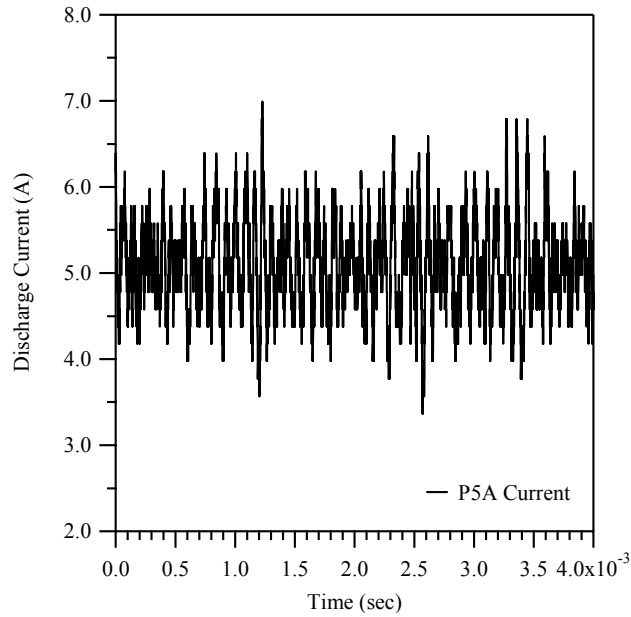


**Figure 6** – The P5-A discharge current at the 300 V, 4.92 A operating condition at a nominal pumping speed of 240 kl/s:  $4.6 \times 10^{-4}$  Pa ( $3.5 \times 10^{-6}$  Torr).

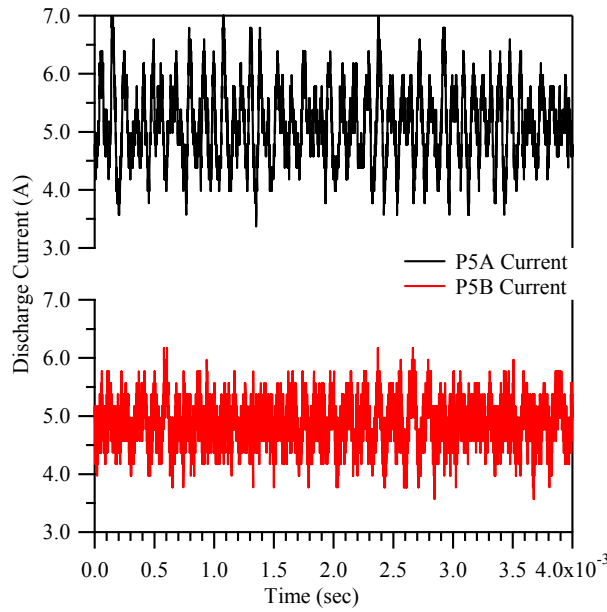


**Figure 7** – Cluster discharge current with the P5-A operating at 300 V, 5.14 A and the P5-B operating at 300 V, 4.96 A. The measurements are taken at a nominal pumping speed of 240 kl/s:  $7.2 \times 10^{-4}$  Pa ( $5.4 \times 10^{-6}$  Torr).

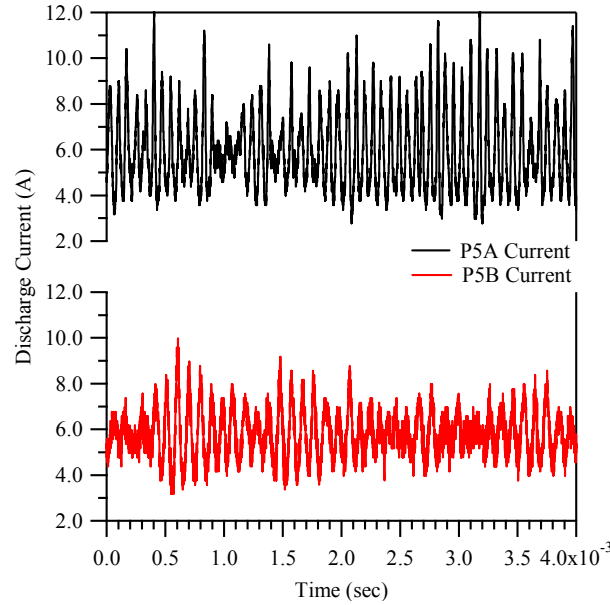


**Figure 8** – Cluster discharge current with the P5-A operating at 300 V, 5.76 A and the P5-B operating at 300 V, 5.68 A. The measurements are taken at a nominal pumping speed of 70 kl/s:  $3.7 \times 10^{-3}$  Pa ( $2.8 \times 10^{-5}$  Torr)

#### IV. Discussion

Figures 9 and 10 present the anode efficiency and anode specific impulse of the P5-A, respectively. Since the performance parameters of the P5-A and P5-B are similar, only the anode efficiency and specific impulse of the P5-A are shown. Figure 9 shows that, in general, for a given flow rate the anode efficiency increases with discharge voltage until a maximum is reached. Any further increase in voltage has little effect on the efficiency or causes it to decrease. Increasing the anode mass flow rate from 5.25 mg/s to 10.46 mg/s increases the maximum efficiency. At an anode flow rate of 5.25 mg/s with a backpressure of  $9.1 \times 10^{-6}$  Torr, the anode efficiency decreases with increasing discharge voltage. At this condition the ingested flow rate, calculated with kinetic theory using an assumed temperature of 300 K, is 0.8% of the injected anode flow, the highest ratio of injected flow to ingested flow. What appears to happen is that the increase in discharge current caused by background gas ingestion overwhelms the increase in thrust. Therefore, more power is supplied to the thruster, but the beam jet power does not increase as quickly. Unfortunately, the physical mechanisms that govern how the ingested particles interact with the ionization and acceleration process (which leads to the decrease in anode efficiency) are not understood. Figure 10 presents the anode specific impulse of the P5-A. For each anode flow rate, the specific impulse increases continually with increasing discharge voltage. These observations agree well with the performance of the original UM/AFRL P5 Hall thruster and theory.<sup>12</sup>

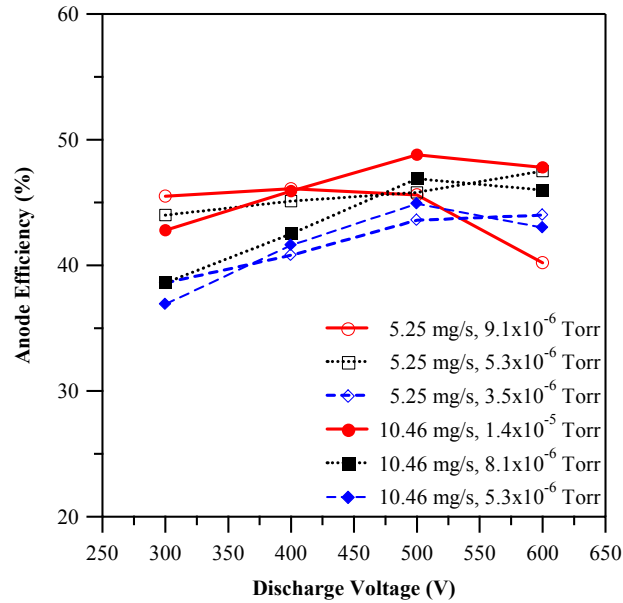


Figure 9 – The P5-A anode efficiency versus discharge voltage.

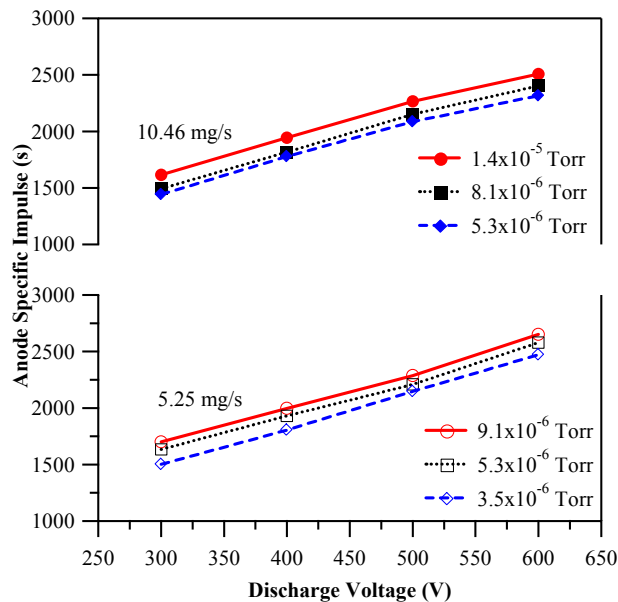


Figure 10 – The P5-A anode specific impulse versus discharge voltage.

As shown in Figures 3 and 4, the performance of a Hall thruster is affected by the facility backpressure. The random flux of neutral particles are ingested into the discharge chamber. The ingested background gas increases the thrust, discharge current, and amplitude of the discharge current oscillations of the thruster for a given operating condition. The ingested background particles are ionized in the discharge channel and accelerated downstream, artificially increasing the measured thrust. In addition, oscillations of the discharge current and electron collisions with the ingested neutrals enhance the electron mobility across the magnetic field. The increase in the number of electrons that reach the anode increases the discharge current. Several studies have attempted to explain the

phenomena behind this behavior.<sup>3, 14</sup> One approach that is routinely applied to correct performance data for ingested flow is to extrapolate thrust versus pressure data to zero background pressure.<sup>15</sup>

With the thrust data collected across the P5 Hall thruster operating range at three operating pressures and two anode flow rates we look to quantify the effects of the ingestion of neutral background gas at the Hall thruster exit plane. From this, we attempt to develop a tool to correct the performance of a Hall thruster operated at elevated facility backpressure. The approach taken in this paper to correct the thrust measurement of a thruster operated at elevated backpressure is to account for the thrust increment that may be provided by the ingested gas that is accelerated downstream.<sup>16</sup> Knowing the open area of the discharge channel, the facility backpressure and assuming the background gas has reached a thermal equilibrium temperature of 300 K with the chamber walls we can use kinetic theory to calculate the mass flow rate of ingested background gas.<sup>4</sup> Note that if the discharge extends significantly past the exit plane of the thruster then the effective area of the discharge is incorrect. Next, assume that the Hall thruster has an ionization efficiency of 80% for neutral propellant that originates from the anode.<sup>17, 18</sup> However, the ionization probability of an ingested particle is much higher because any particle that makes it through the ionization region on the way into the channel must travel through the ionization region a second time as it exits the channel. The particles are accelerated at the operating voltages measured by Gulczinski with an energy analyzer on the P5 Hall thruster.<sup>19</sup> The thrust increment created by ingested background neutrals is now calculated and used to correct the thrust measurements. The percent difference is calculated between the corrected thrust measurements taken at 140 kl/s and the thrust measurements taken at 240 kl/s.

Figures 11 and 12 show the thrust percent differences for anode flow rates of 5.25 mg/s and 10.46 mg/s, respectively. The uncorrected data show that the thrust measurements taken at a pumping speed of 140 kl/s are as much as 8% greater than the thrust measurements taken at a pumping speed of 240 kl/s. The corrected data show that the “random flux” correction method does not adequately account for the phenomena created by elevated backpressure.

To truly correct for the effect of ingested background gas on the performance of a Hall thruster, the composition of the plume must be characterized at each backpressure pressure. As the backpressure increases, a greater number of multiply-charged ions may be created in the discharge chamber.<sup>20</sup> The percentage of multiply-charged ions must be quantified to correct the thrust because the exit velocity of each ion depends on the ion charge state. In the future, we will use an **ExB** probe to make direct measurements of the species-dependent ion energy distributions in the plume of the monolithic thruster. In addition, the plume divergence angle is strongly dependent on the facility backpressure.<sup>21, 22</sup> A change in the plume divergence angle also affects the thrust. In subsequent tests, we will use Faraday probe measurements to determine the plume divergence angle of the monolithic thruster.

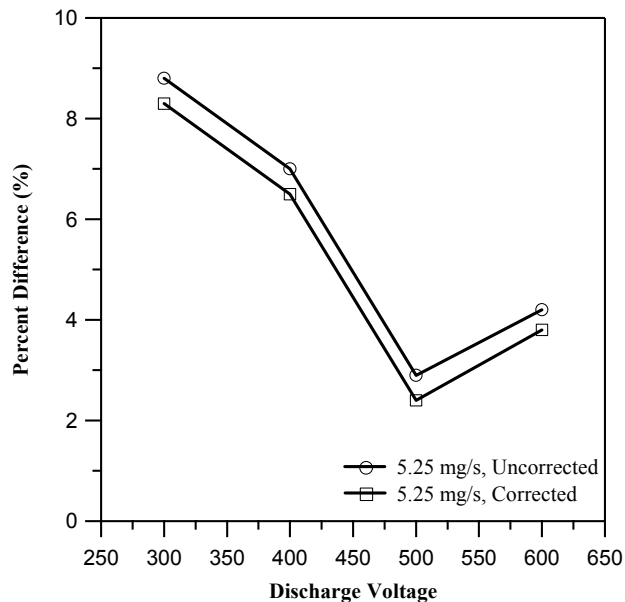


**Figure 11** – Percent difference in measured thrust of the P5-A at nominal pumping speeds of 140 kl/s and 240 kl/s for an anode flow rate of 5.25 mg/s.

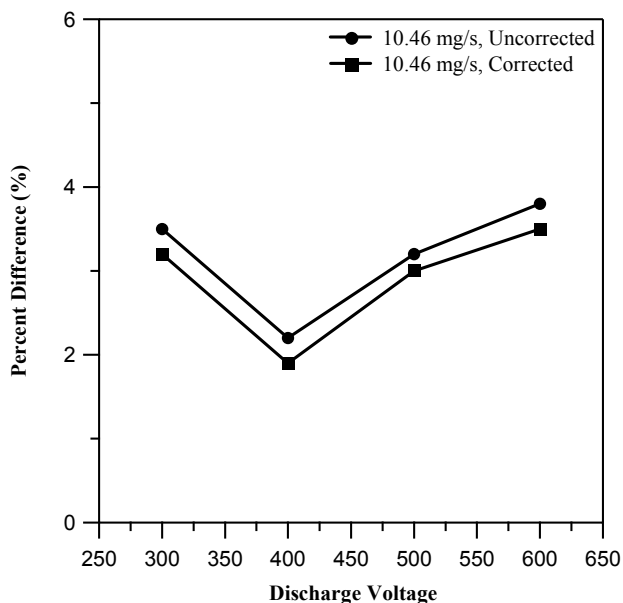


**Figure 12** – Percent difference in the measured thrust of the P5-A at nominal pumping speeds of 140 kl/s and 240 kl/s for an anode flow rate of 10.46 mg/s.

To use a cluster of Hall thrusters to create a high-power electric propulsion system, it is imperative to understand how the thrust of each engine contributes to that of the cluster. Figures 13 and 14 compare the addition of the thrust of the P5-A and P5-B to the thrust of the cluster. All of the cluster thrust measurements are greater than the addition of the two monolithic thrusters. This is because the cluster introduces twice the mass flow rate of propellant into the facility, nearly doubling the backpressure in comparison to the same operating condition for a single thruster. Therefore, the thrust augmentation due to ingestion is greater for each element of the cluster than for the monolithic test case. Thus, the cluster thrust measurements are greater than the addition of the two monolithic thrust measurements. In addition, the cluster shows a much larger enhancement in thrust with increasing facility backpressure than was seen with the monolithic thruster. The thrust of the cluster may also be enhanced by plume interaction. Beal found that the electric field in the plume of an adjacent thruster turns divergent beam ions axially.<sup>19</sup> This focusing of ions leads to a decrease in the plume divergence angle and thus an increase in thrust.

Figure 15 shows the thrust percent difference between measured cluster thrust and the thrust that results from the addition of the measured thrust of the monolithic thrusters for the flow rates of 5.25 and 10.46 mg/s at the three pumping speeds. The thrust percent difference is calculated by subtracting the sum of the thrust of the P5-A and P5-B from the thrust of the cluster and then dividing by the sum of the thrust of the P5-A and P5-B. There is not a large change in the thrust percent difference as the discharge voltage increases. The percent difference in thrust for the 10.46 mg/s anode flow rate varies from 11% to 16%, where the monolithic operating pressure varies from  $5.3 \times 10^{-6}$  Torr to  $1.4 \times 10^{-5}$  Torr and the cluster operating pressure varies from  $8.9 \times 10^{-6}$  Torr to  $2.8 \times 10^{-5}$  Torr. This is greater than the percent difference in thrust for the 5.25 mg/s anode flow rate, which varies from 0% to 6%, where the monolithic operating pressure varies from  $3.5 \times 10^{-6}$  Torr to  $9.1 \times 10^{-6}$  Torr and the cluster operating pressure varies from  $5.4 \times 10^{-6}$  Torr to  $1.5 \times 10^{-5}$  Torr. These differences exist because the facility backpressure is greatest at the 10.46 mg/s anode flow rate, thus the thrust augmentation due to ingestion is greatest. For a given flow rate, the thrust percent difference increases as the operating pressure decreases. This is primarily because the thrust of either the P5-A or P5-B operated alone decreases with backpressure faster than the thrust of the cluster decreases with pressure.

A plot of cluster anode efficiency as a function of voltage is shown in Figure 16. In general, the cluster anode efficiency increases with discharge voltage for a given anode flow rate. However, at an anode flow rate of 5.25 mg/s with an operating pressure of  $1.5 \times 10^{-5}$  Torr, the cluster anode efficiency decreases with increasing discharge voltage. The same behavior is seen in Fig. 9 for the P5-A. The ingested flow rate, calculated with kinetic theory, is only 1.3% of the injected anode flow at this condition. This condition has the highest ratio of injected flow to

ingested flow of the cluster measurements. As is shown with the monolithic thruster, the increase in discharge current overwhelms the increase in thrust. Thus, the ratio of supplied power to beam jet power decreases. This can be seen in the data presented in Table 4. This results in the decrease in anode efficiency as discharge voltage of the cluster increases. The cluster anode efficiency is greatest at the 10.46 mg/s anode flow rate, which is the same behavior seen in the monolithic anode efficiency. The anode efficiency increases with facility backpressure because the background gas ingestion artificially increases the thrust at a rate that is greater than the increase in power supplied to the thruster since the discharge current increases with backpressure. This trend is also apparent in the monolithic thruster efficiency.

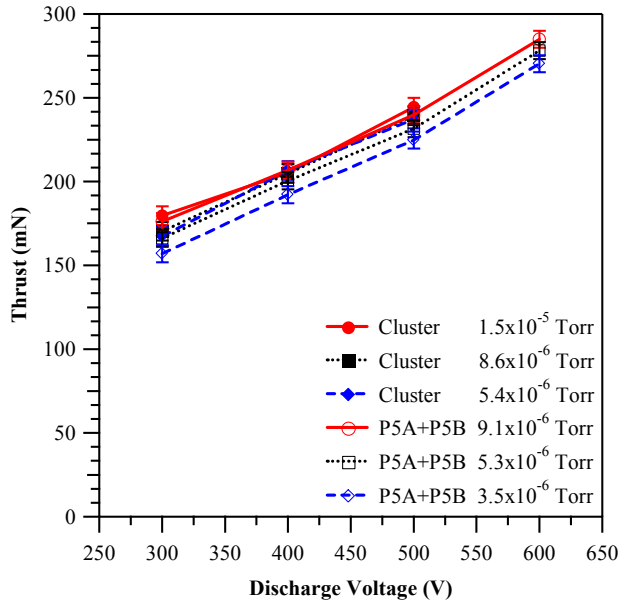
Figure 17 shows the cluster specific impulse. The cluster specific impulse increases continually as the discharge voltage increases. The same trend is observed in the specific impulse of the monolithic thrusters. The cluster specific impulse appears to increase slightly with anode flow rate for the measured points. This is opposite of the trend seen with the monolithic thrusters. The specific impulse is a function of the exit velocity of the particles. The exit velocity of the ions is determined by the discharge voltage. The cluster specific impulse appears to increase as the facility backpressure increases for a constant discharge voltage. This is because the ingested background gas increases the thrust, but the ingested flow is not accounted for in the calculation of the anode specific impulse.

The differences in facility operating pressure make it difficult to compare the performance of the monolithic thruster and the cluster at the same thruster operating condition. As shown in Table 1, the chamber operating pressure with the monolithic thruster operating in the facility at a nominal pumping speed of 70 kl/s is approximately the same as the operating pressure with the cluster operating in the facility at a nominal pumping speed of 140 kl/s. Thus, comparisons between monolithic and cluster data at these conditions may be independent of facility operating pressure.

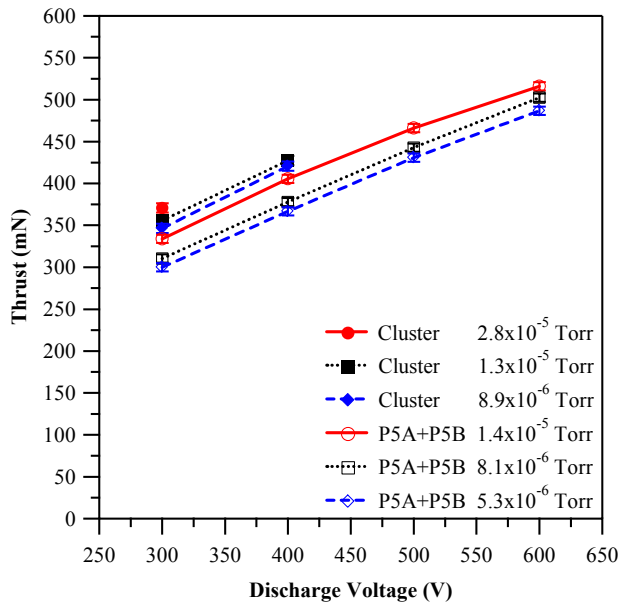
Figures 18 - 20 show the thrust, specific impulse, and anode efficiency of the monolithic thruster operating in the facility at a nominal pumping speed of 70 kl/s and the cluster operating at a nominal pumping speed of 140 kl/s. As indicated in each figure, the operating pressure of the monolithic thruster and the cluster is approximately the same for anode flow rates of 5.25 mg/s and 10.46 mg/s. Figure 18 shows that at the 5.25 mg/s flow rate, the sum of the thrust of the monolithic thrusters is approximately equal the thrust of the cluster. However, at the 10.46 mg/s flow rate the cluster thrust is greater than that of the monolithic thrusters. The fact that the thrust of the cluster is greater than the sum of the thrust of the monolithic thrusters may be caused by each cluster element elevating the operating pressure in the immediate vicinity of the adjacent thruster. The elevated operating pressure also affects the cluster specific impulse and anode efficiency at the 10.46 mg/s anode flow rate.

Figure 19 shows that at the 5.25 mg/s anode flow rate the specific impulse of the cluster is approximately the same as that of the monolithic thruster. However, at the 10.46 mg/s flow rate, the specific impulse of the cluster is approximately 250 seconds greater than that of the monolithic thruster. As discussed earlier, the increase in cluster specific impulse is caused by not accounting for the ingested background gas in the calculation of specific impulse.

Figure 20 shows that at the 5.25 mg/s anode flow rate the anode efficiency of the cluster is approximately the same as that of the monolithic thruster, within the error of the measurement. At the 10.46 mg/s anode flow rate, the cluster anode efficiency is lower than the anode efficiency of the monolithic thruster. As explained earlier, the power supplied to the thruster increases faster than the jet power of the beam because of the ingested background gas, which leads to a decrease in the anode efficiency.



**Figure 13** – Cluster thrust measurements in comparison to the addition of the monolithic thrust for an anode flow rate of 5.25 mg/s at nominal pumping speeds of 70 kl/s, 140 kl/s, and 240 kl/s.



**Figure 14** – Cluster thrust measurements in comparison to the addition of the monolithic thrust at an anode flow rate of 10.46 mg/s at nominal pumping speeds of 70 kl/s, 140 kl/s, and 240 kl/s.

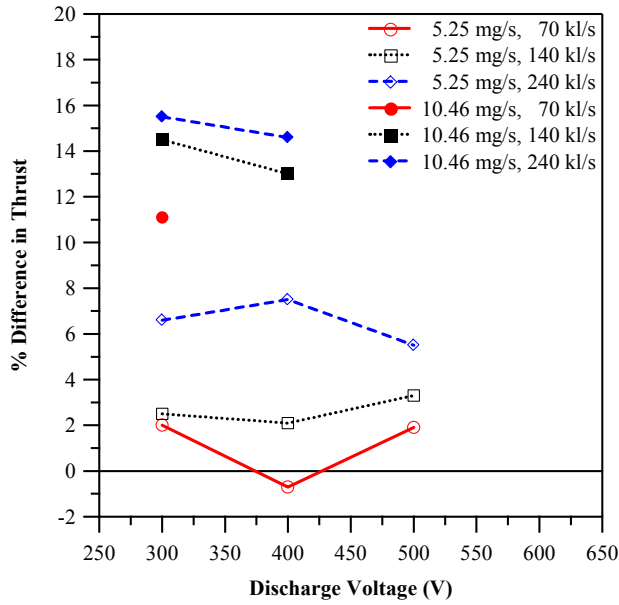


**Figure 15** – Percent difference between measured cluster thrust and the addition of the measured monolithic thrust at anode flow rates of 5.25 mg/s and 10.46 mg/s at nominal pumping speeds of 70 kl/s, 140 kl/s, and 240 kl/s.

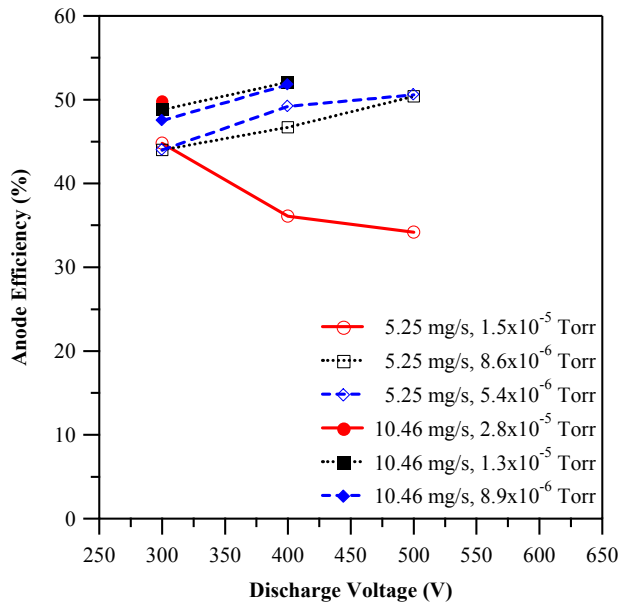


**Figure 16** – Cluster anode efficiency versus discharge voltage at nominal pumping speeds of 70 kl/s, 140 kl/s, and 240 kl/s.

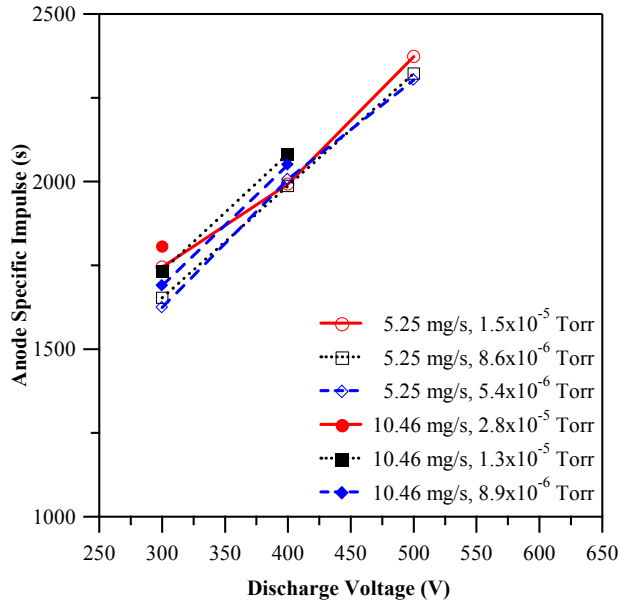


**Figure 17** – Cluster anode specific impulse versus discharge voltage at nominal pumping speeds of 70 kl/s, 140 kl/s, and 240 kl/s.

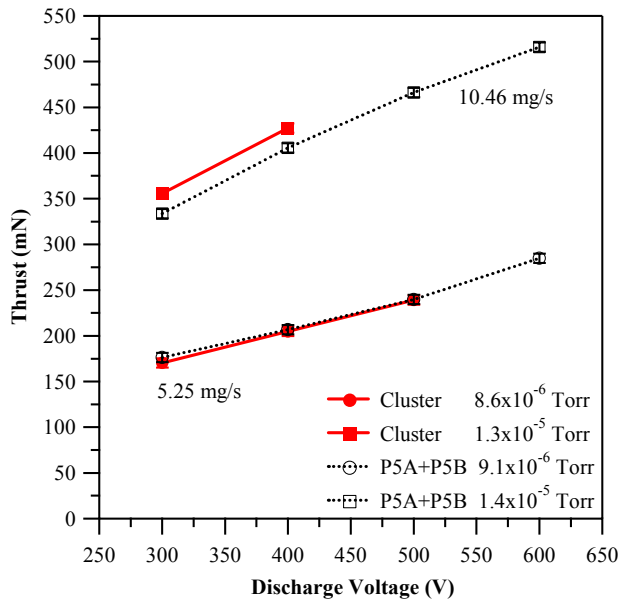


**Figure 18** – Thrust versus discharge voltage for the sum of the P5A and P5B at a nominal pumping speed of 70 kl/s, and the thrust of the cluster at nominal pumping speed of 140 kl/s.

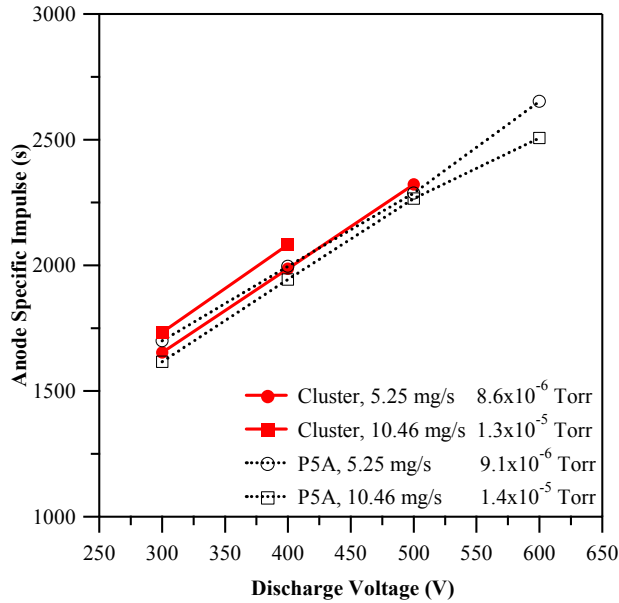


**Figure 19** – Specific impulse versus discharge voltage for the sum of the P5A at a nominal pumping speed of 70 kl/s and the cluster at a nominal pumping speed of 140 kl/s.

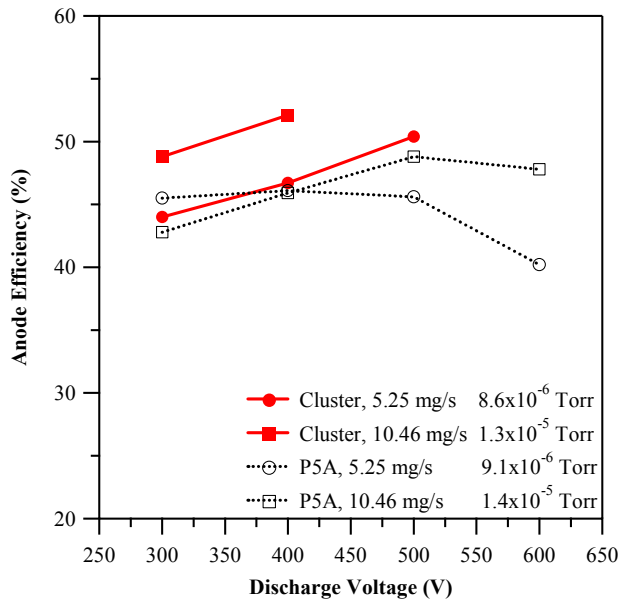


**Figure 20** – Anode efficiency versus discharge voltage for the sum of the P5A at a nominal pumping speed of 70 kl/s, and the cluster at a nominal pumping speed of 140 kl/s.

## V. Conclusion

Analysis of the monolithic thrust measurements shows that as the facility backpressure increases, the thruster discharge current and thrust increase as more background xenon gas is ingested into the thruster discharge chamber, as is expected. The percent difference in thrust for the 10.46 mg/s anode flow rate varies from 11% to 16% as the

operating pressure varies from  $5.3 \times 10^{-6}$  Torr to  $2.8 \times 10^{-5}$  Torr. This is greater than the percent difference in thrust for the 5.25 mg/s anode flow rate, which varies from 0% to 6% as the operating pressure varies from  $3.5 \times 10^{-6}$  Torr to  $1.5 \times 10^{-5}$  Torr. The difference between the two flow rates is caused by the ingestion of background gas and thus, the difference in thrust between the cluster and the addition of the monolithic thrusters increases as the operating pressure decreases. The efficiency of the cluster shows the same trends as the monolithic thruster. The efficiency values of the cluster are slightly greater than those of the monolithic thruster. The difference appears to be caused by the ingested background gas. The specific impulse of the cluster increases with discharge voltage. However, the specific impulse increases with facility backpressure, which was not seen with the monolithic thruster. This is possibly due to the fact that the calculation of specific impulse does not take the ingested background gas into account.

Comparison of the performance characteristics of the cluster and the monolithic thruster at conditions of nearly equal operating pressure shows that for the 5.25 mg/s anode flow rate the cluster thrust is simply the addition of the thrust of the two monolithic thrusters. In addition, the anode efficiency and specific impulse are approximately equal to that of the monolithic thruster. However, these trends do not hold at the 10.46 mg/s anode flow rate for conditions of equal operating pressure because each cluster element elevates the operating pressure in the immediate vicinity of the adjacent thruster and the effects of ingestion are apparent. This will be verified with a measurement of the operating pressure immediately downstream of the cluster.

A method to correct performance measurements taken at elevated backpressures must take into account the changes in the percentage of multiply-charged ions, ion energy distribution, and plume divergence as the facility backpressure increases. The cluster spacing criterion based on magnetic field in the inner channel appears to be adequate for performance measurements. Further verification of the method requires ion energy and charge state measurements to be made in the plume of the cluster. It may also be possible to move the elements of the cluster closer together without adversely affecting their performance.

### Acknowledgments

The research contained herein was sponsored by the Air Force Office of Scientific Research. (Dr. Mitat Birkan is the contract monitor). We would like to thank Dr. James Haas at AFRL for supplying PEPL with the cluster elements, Mr. Terry Larrow for fabricating the hardware used in this study, Dr. Sergi Khartov at MAI for use of the LaB<sub>6</sub> cathode design, and the departmental technical staff and other graduate students at PEPL for help in maintaining the facilities. We would also like to thank Torsten Stindl of the University of Stuttgart. M. L. R. Walker is supported by the Michigan Space Grant Consortium and the National Science Foundation. The authors are greatly appreciative of this support.

### References

1. Jankovsky, R. S., Jacobson, D., Manzella, D. H., "50 kW Class Krypton Hall Thruster Performance," AIAA-2003-4550, 39<sup>th</sup> Joint Propulsion Conference, Huntsville, AL, July 20-23, 2003.
2. "Project Prometheus," [online] URL: <http://spacescience.nasa.gov/missions/prometheus.htm> [cited 1 May 2004].
3. Semenkin, A., Kim, V., Gorshokov, O., Jankovsky, R., "Development of Electric Propulsion Standards – current status and further activity," IEPC-2001-070, 27<sup>th</sup> International Electric Propulsion Conference, Pasadena, CA, October 15-19, 2001.
4. Randolph, T., Kim, V., Kaufman, H., Kozubsky, K., Zhurin, V., Day, M., "Facility Effects on Stationary Plasma Thruster Testing," IEPC-93-93, 23<sup>rd</sup> International Electric Propulsion Conference, Seattle, WA, September 13-16, 1993.
5. King, L. B., Gallimore, A. D., "Ionic and Neutral Particle Transport Property measurements in the Plume of an SPT-100," AIAA-96-2712, 32<sup>nd</sup> Joint Propulsion Conference, Lake Buena Vista, FL, July 1-3, 1996.
6. Beal, B. E., Gallimore, A. D., "The Effects of Clustering Multiple Hall Thrusters on Plasma Plume Properties," 39<sup>th</sup> Joint Propulsion Conference and Exhibit, Huntsville, AL, July 20-23, 2003.

7. Beal, B. E., *et al.*, "Preliminary Plume Characterization of a Low-Power Hall Thruster Cluster," AIAA-2002-4251, 38<sup>th</sup> Joint Propulsion Conference & Exhibit, Indianapolis, IN, July 7-10, 2002.
8. Beal, B. E., *et al.*, "Energy Analysis of a Hall Thruster Cluster," IEPC-2003-0035, 28<sup>th</sup> International Electric Propulsion Conference, Toulouse, France, March 17-21, 2003.
9. Hargus Jr., W. A., *et al.*, "The Air Force Clustered Hall Thruster Program," AIAA-2002-3678, 38<sup>th</sup> Joint Propulsion Conference & Exhibit, Indianapolis, IN, July 7-10, 2002.
10. Walker, M. L. R., Gallimore, A. D., "Pressure Map of a Facility as a Function of Flow Rate to Study Facility Effects," AIAA-2002-3815, 38<sup>th</sup> Joint Propulsion Conference, Indianapolis, IN, July 7-10, 2002.
11. Dushman, S., *Scientific Foundations of Vacuum Technique*, Vol. 4, Wiley, New York, 1958.
12. Haas, J. M., Gulczinski III, F. S., Gallimore, A. D., "Performance Characteristics of a 5 kW Laboratory Hall Thruster," AIAA-98-3503, 34<sup>th</sup> Joint Propulsion Conference, Cleveland, OH, July 12-15, 1998.
13. Hofer, R. R., Gallimore, A. D., "Recent Results from Internal and Very-Near-Field Plasma Diagnostics of a High Specific Impulse Hall Thruster," IEPC-2003-037, 28<sup>th</sup> International Electric Propulsion Conference, Toulouse, France, March 17-21, 2003.
14. Hofer, R. H., Peterson, P. Y., Gallimore, A. D., "Characterizing Vacuum Facility Backpressure Effects on the Performance of a Hall Thruster," IEPC-01-045, International Electric Propulsion Conference, Pasadena, CA, October 14-19, 2001.
15. de Grys, K., Meckel, N., Callis, G., Greisen, D., Hoskins, A., King, D., Wilson, F., Werthman, L., Khayms, V., "Development and Testing of a 4500 Watt flight Type Hall Thruster and Cathode," IEPC-01-011, 27<sup>th</sup> International Electric Propulsion Conference, Pasadena, CA, October 15-19, 2001.
16. Manzella, D. H., Sankovic, J. M., "Hall Thruster Ion Beam Characterization," AIAA-95-2927, 31<sup>st</sup> Joint Propulsion Conference, San Diego, CA, July 10-12, 1995.
17. Hofer, R. R., Jankovsky, R. S., "A Hall Thruster Performance Model Incorporating the Effects of a Multiply-Charged Plasma," AIAA-2001-3322, 37<sup>th</sup> Joint Propulsion Conference, Salt Lake City, UT, July 8-11, 2001.
18. Zhurin, V. V., Kaufman, H. R., Robinson, R. S., "Physics of closed drift thrusters," *Plasma Source Science and Technology*, Vol. 8, 1999, pp. R1-R20.
19. Gulczinski, F. S., "Examination of the Structure and Evolution of Ion Energy Properties of a 5 kW Class Laboratory Hall Effect Thruster at Various Operational Conditions," Ph.D. Dissertation, University of Michigan, 1999.
20. Zhurin, V., Kahn, J., Kaufman, H., Kozubsky, K., Day, M., "Dynamic Characteristics of Closed Drift Thruster," IEPC-93-095, 23<sup>rd</sup> International Electric Propulsion Conference, Seattle, Washington, September 13-16, 1993.
21. de Grys, K. H., Tilley, D. L., Aadland, R. S., "BPT Hall Thruster Plume Characteristics," AIAA-99-2283, 35<sup>th</sup> Joint Propulsion Conference, Los Angeles, CA, June 20-24, 1999.
22. Walker, M. L. R., Hofer, R. R., Gallimore, A. D., "The Effects of Nude Faraday Probe Design on the Measured Ion Current Density Profile of Hall Thruster Plumes," AIAA-2002-4253, 38<sup>th</sup> Joint Propulsion Conference & Exhibit, Indianapolis, IN, July 7-10, 2002.
23. Walker, M. L. R., Gallimore, A. D., "Hot Flow Pressure Map of a Vacuum Facility as a Function of Flow Rate to Study Facility Effects," IEPC-03-0077, 28<sup>th</sup> International Electric Propulsion Conference, Toulouse, France, 17-21 March 2003.

## Appendix

**Table 2 - P5-A operating conditions**

Pumps	Discharge Voltage (V)	Discharge Current (A)	Anode (mg/s)	Cathode (mg/s)	Inner Magnet Current (A)	Outer Magnet Current (A)	Vc-g (V)	Pressure (Torr-Xe)	Pressure (Pa-Xe)
2	300	5.34	5.25	0.92	2.56	1.43	-16.5	9.1E-06	1.2E-03
2	400	5.46	5.25	0.92	3.14	1.55	-15.4	9.1E-06	1.2E-03
2	500	5.80	5.25	0.92	3.98	1.57	-14.9	9.1E-06	1.2E-03
2	600	7.36	5.25	0.92	3.95	2.71	-14.6	9.1E-06	1.2E-03
2	300	10.24	10.46	0.92	3.06	1.82	-18.2	1.4E-05	1.8E-03
2	400	10.36	10.46	0.92	3.92	2.00	-17.9	1.4E-05	1.8E-03
2	500	10.60	10.46	0.92	4.28	3.00	-17.9	1.4E-05	1.8E-03
2	600	11.02	10.46	0.92	6.25	3.00	-18.6	1.4E-05	1.8E-03
4	300	5.10	5.25	0.92	2.56	1.43	-16.2	5.3E-06	7.1E-04
4	400	5.22	5.25	0.92	3.14	1.55	-16.0	5.3E-06	7.1E-04
4	500	5.38	5.25	0.92	3.98	1.57	-16.7	5.3E-06	7.1E-04
4	600	5.88	5.25	0.92	3.95	2.71	-15.0	5.3E-06	7.1E-04
4	300	9.68	10.46	0.92	3.06	1.82	-17.5	8.1E-06	1.1E-03
4	400	9.76	10.46	0.92	3.92	2.00	-17.3	8.1E-06	1.1E-03
4	500	9.94	10.46	0.92	4.28	3.00	-17.0	8.1E-06	1.1E-03
4	600	10.52	10.46	0.92	6.25	3.00	-17.3	8.1E-06	1.1E-03
7	300	4.92	5.25	0.92	2.56	1.43	-16.4	3.5E-06	4.6E-04
7	400	5.04	5.25	0.92	3.14	1.55	-16.0	3.5E-06	4.6E-04
7	500	5.34	5.25	0.92	3.98	1.57	-15.2	3.5E-06	4.6E-04
7	600	5.84	5.25	0.92	3.95	2.71	-14.0	3.5E-06	4.6E-04
7	300	9.46	10.46	0.92	3.06	1.82	-16.8	5.3E-06	7.1E-04
7	400	9.56	10.46	0.92	3.92	2.00	-16.7	5.3E-06	7.1E-04
7	500	9.74	10.46	0.92	4.28	3.00	-16.5	5.3E-06	7.1E-04
7	600	10.44	10.46	0.92	6.25	3.00	-17.8	5.3E-06	7.1E-04

Table 3 - P5-B operating conditions

Pumps	Discharge Voltage (V)	Discharge Current (A)	Anode (mg/s)	Cathode (mg/s)	Inner Magnet Current (A)	Outer Magnet Current (A)	Vc-g (V)	Pressure (Torr-Xe)	Pressure (Pa-Xe)
2	300	5.42	5.25	0.92	2.56	1.43	-16.5	9.2E-06	1.2E-03
2	400	5.48	5.25	0.92	3.14	1.55	-15.4	9.2E-06	1.2E-03
2	500	5.74	5.25	0.92	3.98	1.57	-14.9	9.2E-06	1.2E-03
2	600	6.64	5.25	0.92	3.95	2.71	-14.6	9.2E-06	1.2E-03
2	300	10.52	10.46	0.92	3.06	1.82	-18.2	1.5E-05	2.0E-03
2	400	10.80	10.46	0.92	3.92	2.00	-17.9	1.5E-05	2.0E-03
2	500	10.64	10.46	0.92	4.28	3.00	-17.9	1.5E-05	2.0E-03
2	600	11.02	10.46	0.92	6.25	3.00	-18.6	1.5E-05	2.0E-03
4	300	5.06	5.25	0.92	2.56	1.43	-16.2	5.3E-06	7.1E-04
4	400	5.02	5.25	0.92	3.14	1.55	-16.0	5.3E-06	7.1E-04
4	500	5.20	5.25	0.92	3.98	1.57	-16.7	5.3E-06	7.1E-04
4	600	5.66	5.25	0.92	3.95	2.71	-15.0	5.3E-06	7.1E-04
4	300	9.66	10.46	0.92	3.06	1.82	-17.5	8.1E-06	1.1E-03
4	400	9.60	10.46	0.92	3.92	2.00	-17.3	8.1E-06	1.1E-03
4	500	9.68	10.46	0.92	4.28	3.00	-17.0	8.1E-06	1.1E-03
4	600	10.34	10.46	0.92	6.25	3.00	-17.3	8.1E-06	1.1E-03
7	300	4.98	5.25	0.92	2.56	1.43	-16.4	3.5E-06	4.6E-04
7	400	4.98	5.25	0.92	3.14	1.55	-16.0	3.5E-06	4.6E-04
7	500	5.12	5.25	0.92	3.98	1.57	-15.2	3.5E-06	4.6E-04
7	600	5.60	5.25	0.92	3.95	2.71	-14.0	3.5E-06	4.6E-04
7	300	9.44	10.46	0.92	3.06	1.82	-16.8	5.3E-06	7.1E-04
7	400	9.40	10.46	0.92	3.92	2.00	-16.7	5.3E-06	7.1E-04
7	500	9.50	10.46	0.92	4.28	3.00	-16.5	5.3E-06	7.1E-04
7	600	10.18	10.46	0.92	6.25	3.00	-17.8	5.3E-06	7.1E-04

**Table 4 – Cluster operating conditions**

<b>Pumps</b>	<b>Discharge Voltage (V)</b>	<b>P5A Discharge Current (A)</b>	<b>P5B Discharge Current (A)</b>	<b>Anode (mg/s)</b>	<b>Cathode (mg/s)</b>	<b>Inner Mag. Current (A)</b>	<b>Outer Mag. Current (A)</b>	<b>Pressure (Torr-Xe)</b>	<b>Pressure (Pa-Xe)</b>
2	300	5.76	5.68	5.25	0.92	2.56	1.43	1.5E-05	2.0E-03
2	400	6.94	6.94	5.25	0.92	3.14	1.55	1.5E-05	2.0E-03
2	500	8.26	8.38	5.25	0.92	3.98	1.57	1.5E-05	2.0E-03
2	300	11.08	10.90	10.46	0.92	3.06	1.82	2.8E-05	3.7E-03
2	400	14.54	11.06	10.46	0.92	3.92	2.00	2.8E-05	3.7E-03
4	300	5.24	5.22	5.25	0.92	2.56	1.43	8.6E-05	1.1E-03
4	400	5.34	5.34	5.25	0.92	3.14	1.55	8.6E-05	1.1E-03
4	500	5.42	5.40	5.25	0.92	3.98	1.57	8.6E-05	1.1E-03
4	300	10.32	10.34	10.46	0.92	3.06	1.82	1.3E-05	1.7E-03
4	400	10.48	10.48	10.46	0.92	3.92	2.00	1.3E-05	1.7E-03
7	300	5.14	4.96	5.25	0.92	2.56	1.43	5.4E-06	7.2E-04
7	400	5.26	5.06	5.25	0.92	3.14	1.55	5.4E-06	7.2E-04
7	500	5.36	5.24	5.25	0.92	3.98	1.57	5.4E-06	7.2E-04
7	300	10.14	10.02	10.46	0.92	3.06	1.82	8.9E-06	1.2E-03
7	400	10.26	10.14	10.46	0.92	3.92	2.00	8.9E-06	1.2E-03
7	500	12.92	11.32	10.46	0.92	4.28	3.00	8.9E-06	1.2E-03